The system Pd–Fe–Ni–S at 900 and 725°C

EMIL MAKOVICKY

Department of Mineralogy, Geological Institute, University of Copenhagen, 1350 Copenhagen, Denmark

AND

SVEN KARUP-MØLLER

Institute of Mineral Industry, Technical University of Denmark, 2800 Lyngby, Denmark

Abstract

The system Pd–Fe–Ni–S was studied at 900 and 725°C by means of dry condensed charges. At both temperatures it is dominated by the phase relationships involving sulphide melt. Pd–Fe–Ni alloys with broad miscibility primarily coexist with the melt; they are relatively enriched in Pd, whereas the associated melt is enriched in Ni. With decreasing temperature the melt recedes from Fe-rich regions. The incompatibility of PdS (extensive solid solution with Ni) and *mss* at 900°C is replaced by their co-crystallization (± disulphide(s) of Ni,Fe or ± sulphide melt) at 725°C. The Ni/Fe ratio in the melt changes regularly against that in *mss* with increasing S fugacity and Pd contents in these two phases. $(Ni,Fe)_{3\pm x}S_2$ and Pd_4S play important roles at 725°C. The data offer an array of distribution coefficients and solubility values suitable for geological interpretations.

KEYWORDS: Pd–Fe–Ni–S system, platinum-group elements, palladium, sulphide melt.

Introduction

THE quaternary phase system Pd–Fe–Ni–S represents one of the most important phase systems for understanding the formation of deposits of platinum-group elements. Palladium is often the principal platinum-group metal in PGE deposits and braggite (Pd,Pt,Ni)S its principal mineral. Pentlandite often coexists with Pd-bearing phases in ores and is known to accept Pd in solid solution. The bulk composition of sulphide ores commonly lies close to the solid-solution field of pyrrhotite. The role of sulphide melt, with a composition belonging essentially to this phase system is considered in most theories on the formation of PGE deposits. Although late-stage processes may ultimately determine the resulting chemistry and mineralogy of palladium in many deposits, processes dictated by the solidus and subsolidus behaviour in the system Pd–Fe–Ni–(± Cu)–S may be responsible for the bulk of PGE mineralogy, as well as for its large-scale ore geology and PGE distribution.

This paper is part of a series of contributions on experimental studies of the mineralogy of PGE performed at the University of Copenhagen and the Danish Technical University and financially supported by the European Union. It contains our final description of the phase system Pd–Fe–Ni–S at 900 and 725°C. Work on this system at 550 and 400°C is in progress and will be reported in a subsequent paper. This paper supersedes Makovicky *et al.* (1990); final results on the partial systems Pd–Ni–S and Pd–Fe–S are contained in Karup-Møller and Makovicky (1993) and Makovicky and Karup-Møller (1993) respectively. Previous relevant phase studies were performed by Distler *et al.* (1977) in the system Pd–Fe–Ni–S, by Skinner *et al.* (1976), Distler (1980), Bryukvin *et al.* (1985), and Makovicky *et al.* (1986, 1988) in the system Pd–Fe–S, and by Kullerud (1963, 1967), Clark and Kullerud (1963), Craig and Kullerud (1969) as well as Kullerud *et al.* (1969), in the system Fe–Ni–S. Our work on the Fe–Ni–S system at 725°C is in press.

Experimental

Two hundred and thirteen 100 mg charges were weighed out from pure elements (freshly filed

Mineralogical Magazine, December 1995, Vol. 59, pp. 685–702

Specpure Ni and Fe rods from Johnson Matthey Ltd., with 20 and 15 ppm metallic impurities, respectively; Pd foil from the same source with max. 25 ppm of metallic impurities and sulphur from Fluka (> 99.999%). They were sealed in evacuated silica glass tubes, preheated at 300°C, and annealed at the desired temperatures for periods up to 15 days. After regrinding and homogenization, they were pelletized under a pressure of 4000 kg/cm^2, resealed and annealed for up to 21 days. The choice of annealing temperatures was made on the basis of the published bounding binary and ternary systems of the four-component system Pd–Fe–Ni–S.

The quenched products were studied in reflected light and by means of microprobe analyses. A JEOL Superprobe 733 was used in wavelength-dispersive mode, with an on-line correction program supplied by JEOL. Ni metal, Pd metal, and natural $CuFeS_2$ were used as standards. Wavelengths employed were Ni-$K\alpha$, Fe-$K\alpha$, Pd-$L\alpha$ and S-$K\alpha$, excitation voltage was 20 kV, sample current 30 nA and counting times up to 20 sec. Generally about ten measurements were taken on each phase present. Tables of microprobe data are available as an appendix to the EEC report by Makovicky *et al.* (1990); selected important runs are summarized in Table 1 (deposited; copies available from the Editor on request).

Boundary systems, Ni–S and Pd–S, were studied by Hansen and Anderko (1958), Kullerud and Yund, (1962), Elliott (1965), Shunk (1969), Arnold and Malik (1975). In agreement with this literature the Pd sulphides are denoted as PdS, $Pd_{2.2}S$, $Pd_{2.8}S$ and Pd_4S. The sulphides PdS, NiS_2, FeS_2, as well as the S-poor end-members NiS and FeS were assumed to be stoichiometric and used as internal standards. The detection limits are < 0.1 at.% for Fe and Ni, and 0.2 wt.% for Pd), on the basis of pure synthetic phases.

The composition of sulphide melts was studied by analysing, at lower magnifications, 10–20 representative areas of the solidified melt with a sweeping electron beam. The size of the area swept by the beam was always selected according to the grain size of the solidified region and the space available between the crystals of primary solid phases. The $(Ni,Fe)_{3\pm x}S_2$ decomposition products were analysed in a similar manner. For these measurements, standards were sampled with a sweeping electron beam as well.

Phase relations at 900°C

The boundary systems. The boundary systems Pd–Fe–S, Pd–Ni–S and Fe–Ni–S offer the best insight into the relatively simple phase relations in the quaternary system Pd–Fe–Ni–S at 900°. In the system Fe–Ni–S, Kullerud (1963) found at 900°C an uninterrupted solid solution $Fe_{1-x}S$–$Ni_{1-x}S$, the so-called mono-sulphide solid solution (abbreviated as *mss*), a sulphide melt that reaches from the Ni-rich side of this system far towards Fe-rich compositions (53 wt.% Fe *vs.* 18 wt.% Ni), and NiS_2 dissolves up to 5.5 wt.% Fe. The entire alloy field is occupied by γ-(Fe,Ni), except for the ~ 1 at.% (~1 wt.%) broad field of α-Fe and a similarly narrow two-phase region α–γ (Kubaschewski, in Massalski, 1986). Only nearly pure troilite, FeS, coexists with the (Fe,Ni) alloy; the rest of *mss* coexists with the sulphide melt that is comparatively enriched in Ni.

Our investigations of the Pd–Fe–S and Pd–Ni–S systems were described in detail by Makovicky and Karup-Møller (1993) and Karup-Møller and Makovicky (1993). Fig. 1 shows that the Pd–Ni–S system is characterized by a broad, uninterrupted field of sulphide melt below ~50 at.% (~30 wt.%) S. This melt stretches to much higher and lower sulphur contents than in the Fe–Ni–S system. A similar situation occurs in the Pd–Fe–S system, in which the sulphide melt does not reach the Fe–S boundary. The extreme melt composition, in the alloy–melt–pyrrhotite field, is ~39 at.% (~39.5 wt.%) Fe and 42.4 at.% (24.6 wt.%) S. PdS does not coexist with $Fe_{1-x}S$ or $Ni_{1-x}S$ at this temperature. The PdS–*mss* tie-line is precluded by the two-phase field, sulphide melt–sulphur, in both of the two boundary systems as well as by the association vaesite–melt in the system Pd–Ni–S.

High solubility of Ni in PdS (3.9 at.%; 3.4 wt.%) is contrasted by low solubility of Fe in this phase (0.4 at.%; 0.3 wt.%). Higher maximum S and Pd contents occur in $Fe_{1-x}S$ (~55 at.% (38.7 wt.%) S and 5.5 at.% (12.8 wt.%) Pd) than in $Ni_{1-x}S$ (max 53 at.% (37.3 wt.%) S and 2.1 at.% (4.9 wt.%) Pd).

Alloy-containing associations in the Pd–Fe–Ni–S system. Except for the small two-phase field at the Fe corner of the phase system, no compositional gaps were located in the solid solution field of the γ-(Fe,Ni,Pd) alloy. For detailed mapping of relations between alloy and sulphide melt, a series of charges progressively enriched in Pd was prepared. They were positioned at about 2/3 of the expected distance between the S-free base of the compositional tetrahedron and the S-poor surface of the sulphide melt volume, on lines with the Fe/Ni ratio equal to 1:3, 1:1, 3:1. They parallel a similar series of charges from the partial systems Pd–Ni–S and Pd–Fe–S. The resulting associated alloy and melt compositions are shown in Figs. 2 and 3. The compositional relationships between alloy and melt change throughout the entire compositional field of the melt, but the changes are especially pronounced in the marginal zones along the Ni–Pd and Ni–Fe joins. For each pair of alloy–melt compositions, the alloy is relatively enriched in Pd (especially strongly for the alloy compositions with ~ 33 at.% (~48 wt.%) Pd), and

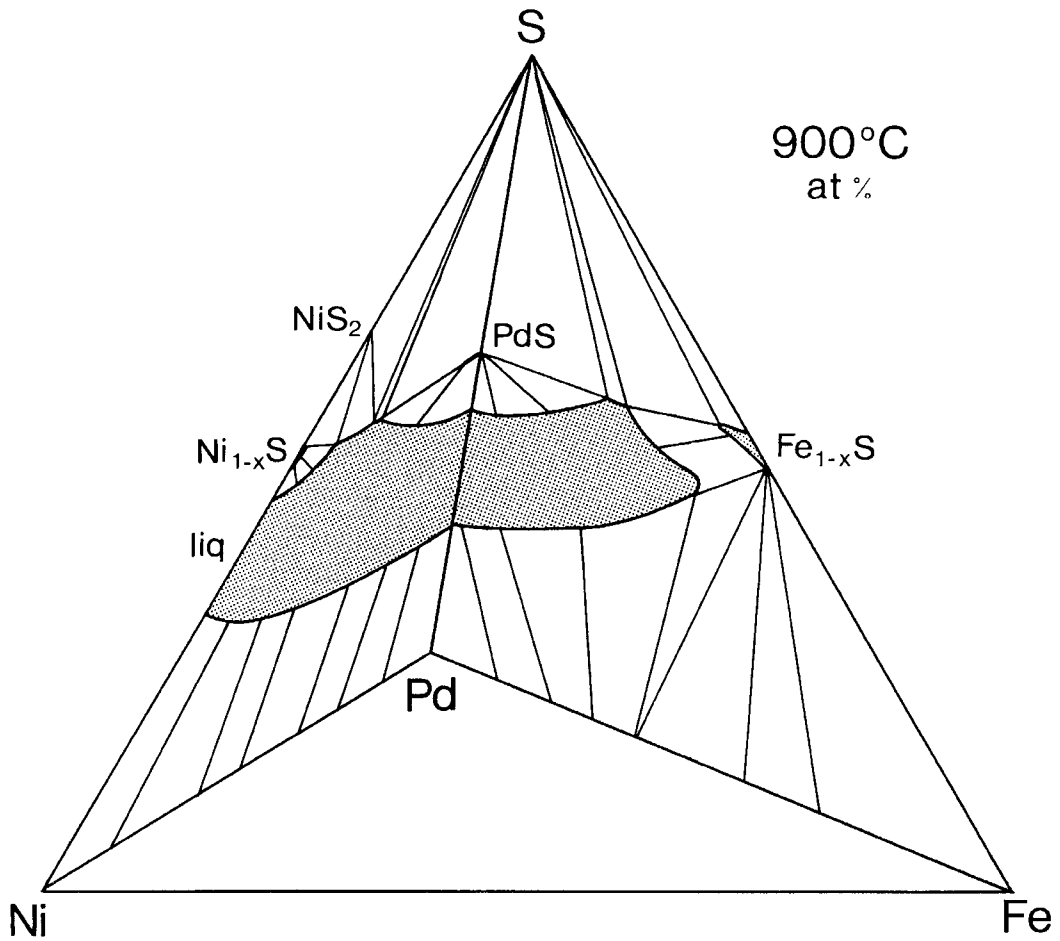

FIG. 1. The systems Pd–Fe–S and Pd–Ni–S at 900°C plotted in the compositional volume Pd–Ni–Fe–S. The compositional field of the sulphide melt is stippled.

has variable Fe/Ni ratios. This relative enrichment decreases towards Pd-rich compositions, representing zero at about 65–70 at.% (78.5–81.3 wt.%) Pd in the alloy. For the most Pd-rich alloys, it is the associated melts that become relatively enriched in Pd.

Approximately within the zone with 10–20 at.% (~20–36 wt.%) Pd in the melt, the sulphide melts undergo progressive enrichment in nickel relative to the associated alloys. This enrichment is parallel to the increase in the Pd contents. Afterwards, the attained Ni/Fe ratio is approximately preserved towards higher Pd contents. The skew is by up to 25 rel.% in favour of Ni. The coexisting, strongly Pd-enriched alloys become progressively enriched in iron in this process. However, for the highest Pd contents their compositions revert towards those of the associated melts (Fig. 3). Thus the compositional development of associated alloys and melts projects in the form of a 'hysteresis loop' in Fig. 3.

In the principal portions of the two-phase field, melt–alloy, the melt–alloy tie-lines lie close to the lines with constant (Ni+Pd)/Fe ratios. For nearly pure Pd–Ni–S melts, the alloy compositions are so enriched in Fe that the respective melt–alloy tie-lines are reoriented parallel to these ratios already within the first 5 at.% Fe in the melt (Fig. 3).

The enrichment/improverishment of the melt by Pd, Ni or Fe with respect to the associated alloy is expressed by distribution coefficients

$$D_i = N_{i(\text{melt})}/N_{i(\text{alloy})},$$

where

N_i = at.% of ith element/Σ (at.% of metals).

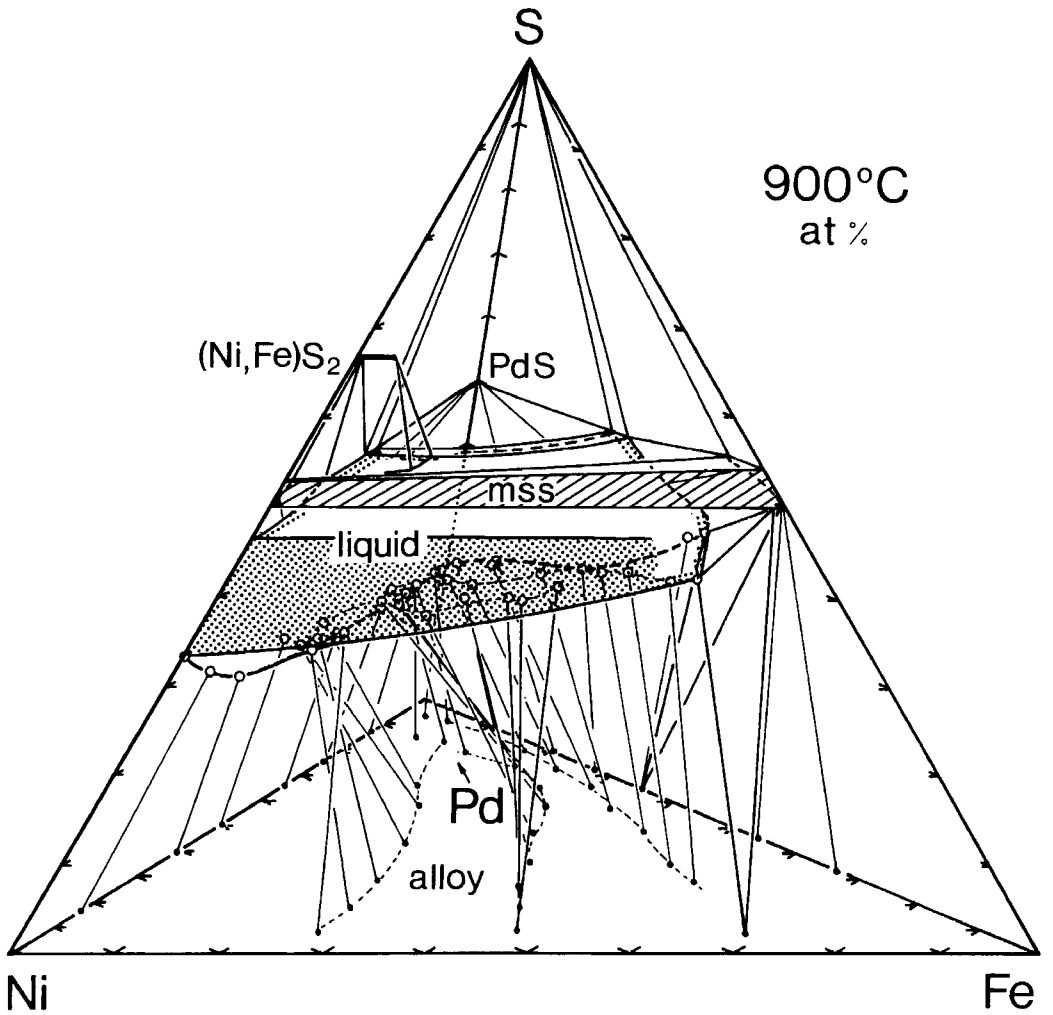

FIG. 2. The system Pd–Fe–Ni–S at 900°C. For the two-phase volume alloy–sulphide melt, a set of typical tie-lines is shown. Mineral phases in this and the following figures are: NiS_2 – vaesite, FeS_2 – pyrite, $Fe_{1-x}S$ – pyrrhotite, Ni_7S_6 – godlevskite, Ni_3S_2 – heazlewoodite, PdS – vysotskite, $Pd_{2.2}S$ – vasilite (Cu-bearing), and Pd_4S – unnamed (Augé and Legendre, 1992).

Distribution coefficients allow deduction of the composition of melts (which have not been preserved) from the compositions of alloys found in ore deposits. Results are written next to the relevant alloy compositions in Fig. 4 and can be used to calculate differentiation of the principal elements during high-temperature crystallization of sulphide melt.

The topography of the low-S surface of the melt is characterized by its progressive sinking, from more than 42 at.% (~ 22 wt.%) S at the Fe-richest edge of its compositional volume, to 20 at.% (~ 8 wt.%) S for the most Pd-rich compositions. The S isochores are approximately parallel to the general direction of the projected melt–alloy tie-lines. The same holds for the most Fe-rich boundary of the melt field.

The pyrrhotite–melt–alloy three-phase field contains pyrrhotite with 50.8–51.1 at.% (~37 wt.%) S, up to 0.1 at.% (0.24 wt.%) Pd and up to 0.9 at.% (1.2 wt.%) Ni. Contents of S, Pd and Ni drop quickly for pyrrhotite–alloy binary associations; for the large part of the compositional range of the two-phase association, *po*–alloy, pyrrhotite does not differ analytically from pure troilite, other than for traces of Ni.

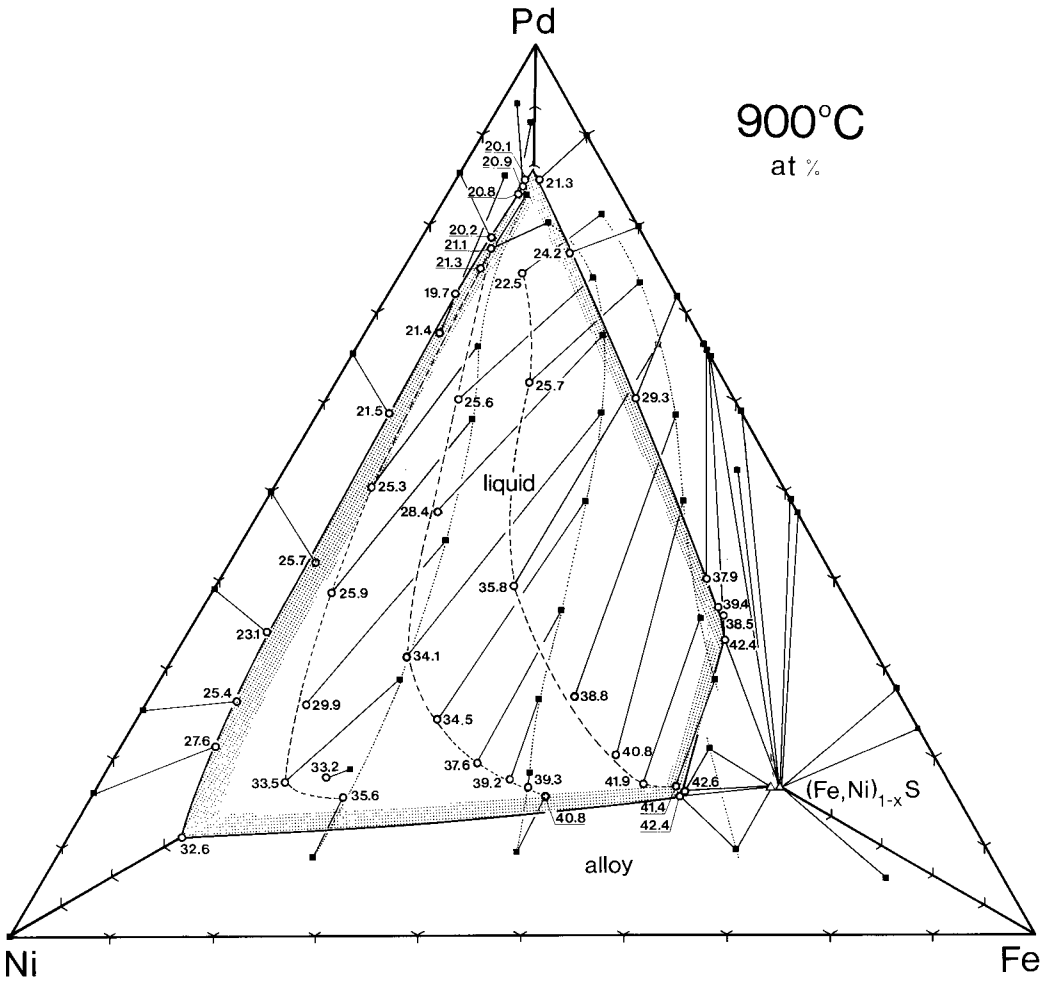

FIG. 3. Parallel projection of alloy-containing associations of the Pd–Fe–Ni–S system at 900°C onto the Pd–Ni–Fe plane. The stippled area outlines the sulphide-melt compositions that coexist with (Pd–Ni–Fe) alloys. The melt compositions are indicated by circles (at.% S in the melt are given), alloy compositions by solid squares, pyrrhotite analyses by triangles. Interrupted lines show the three series of runs described in the text.

The alloy-free sulphide associations in the Pd–Fe–Ni–S system. The Pd-poor portion of the S-rich surface of the sulphide melt volume is occupied mostly by the two-phase association *mss*–melt (Figs. 2 and 5). As it was shown for the boundary systems, the composition of melt is a sensitive function of sulphur fugacity that is expressed through the S contents of the omission solid solution $(Fe,Ni,Pd)_{1-x}S$. A series of runs with the Fe/Ni ratios similar to those used to map the alloy–melt assemblage reveal the complexity of *mss*–melt relationships. For *mss* compositions that are close to stoichiometric (Fe,Ni)S, melt is relatively enriched in Ni along the entire Ni–Fe join, by approximately 10 at.% with respect to the associated *mss*. In the latter, Pd contents vary from traces to 0.2 at.% (~0.5 wt.%). As the amounts of S and Pd in *mss* increase, the tie-lines to the melt rotate clockwise (reducing the amount of Ni enrichment in the melt) and their length increases, reaching progressively towards portions of the melt richer in Pd. For the limiting case, i.e. for the assemblage melt–*mss*–sulphur, Fe/Ni ratios in the melt do not deviate from those in *mss*, and Ni enrichment of the melt does not take place (Fig. 5). Our data yield a range of *mss*/melt distribution coefficients for Ni and Pd that are a function of f_{S_2} (i.e. of S contents in *mss* or melt). These coefficients will be treated in detail elsewhere

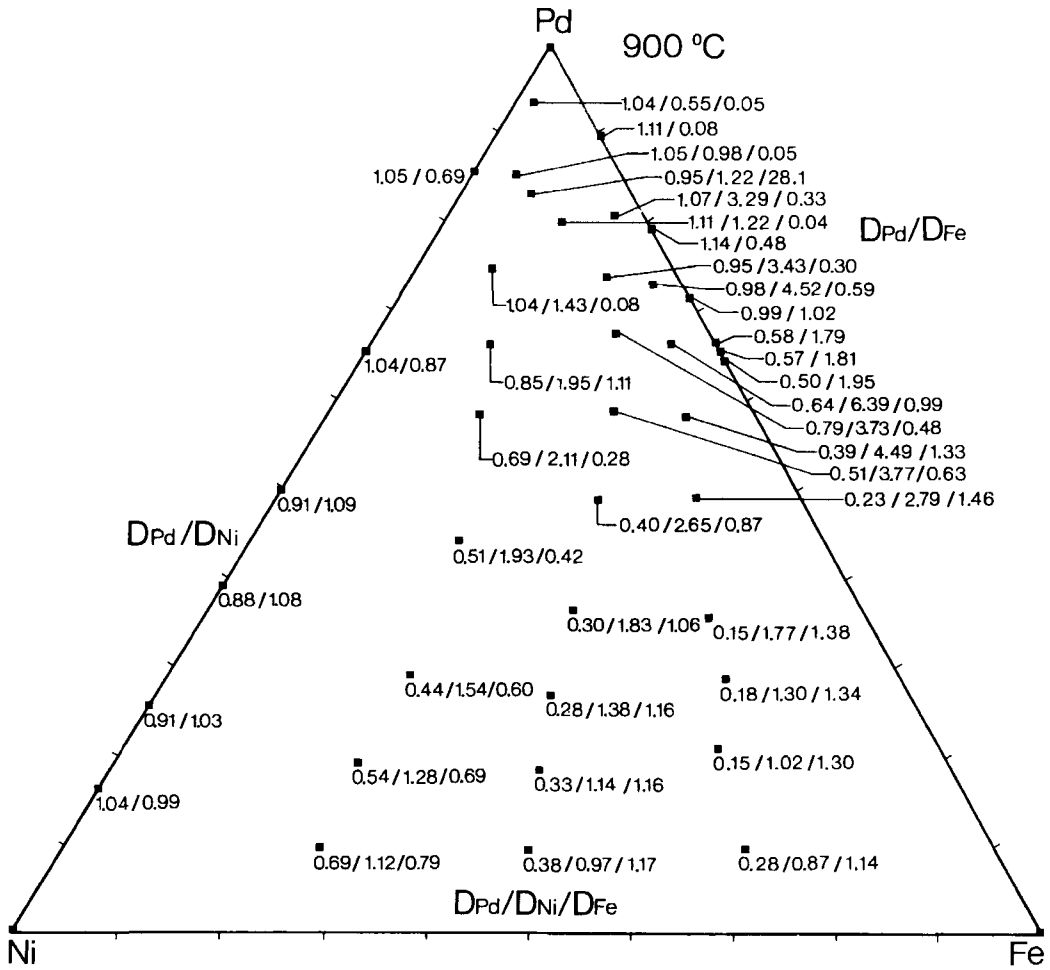

FIG. 4. Melt/alloy distribution coefficients for Pd, Ni and Fe at 900°C inscribed at appropriate alloy compositions.

(Makovicky *et al.* 1994; Barnes *et al.*, 1994, and in preparation).

The binary association sulphide melt–sulphur stretches across the surface of the sulphide melt, interconnecting the compositions $Pd_{23}Ni_{27}S_{50}$ (43.4 wt.% Pd, 28.1 wt.% Ni and 28.4 wt.% S) and $Pd_{21}Fe_{26}S_{53}$ (41.5 wt.% Pd, 27.0 wt.% Fe and 31.5 wt.% S) on the Pd-poor side, and the compositions $Pd_{28}Ni_{22}S_{50}$ (50.7 wt.% Pd, 22.0 wt.% Ni and 27.3 wt.% S) and $Pd_{25}Fe_{22}S_{53}$ (47.6 wt.% Pd, 22.0 wt.% Fe and 30.4 wt.% S) on the Pd-rich side of its composition volume.

The Pd-enriched part of the melt is associated with PdS ± liquid sulphur. The amounts of Ni, Fe and Pd in the melt and in PdS are interrelated. Fe and Ni contents in PdS are a function of both the Fe/(Fe+Ni) and the (Fe+Ni)/Pd ratios (Fig. 5). The tie-lines from the melt are attached laterally to the very elongated but, with respect to Fe, quite narrow compositional field of (Pd,NiFe)S. For the association PdS–melt–sulphur, the typical solubility values are as follows: 0.4 at.% (0.3 wt.%) Fe in PdS from Ni-free runs; 1.0 at.% (0.86 wt.%) Ni and 0.3 at.% (0.24 wt.%) Fe in PdS for the Fe/(Fe+Ni) ratio in melt equal to 0.76 (0.75 by weight); 1.6 at.% (1.2 wt.%) Ni and 0.2 at.% (0.14 wt.%) Fe for this ratio in the melt equal to 0.61 (0.60 by weight), as well as 2.9 at.% (2.5 wt.%) Ni and 0.1 at.% (0.08 wt.%) Fe for this ratio equal to 0.32 (0.33 by weight). The Fe-free charge has 3.9 at.% (3.4 wt.%) Ni in PdS at this temperature.

The only complication in these, more S-rich parts of the Pd–Fe–Ni–S system at 900°C is caused by the

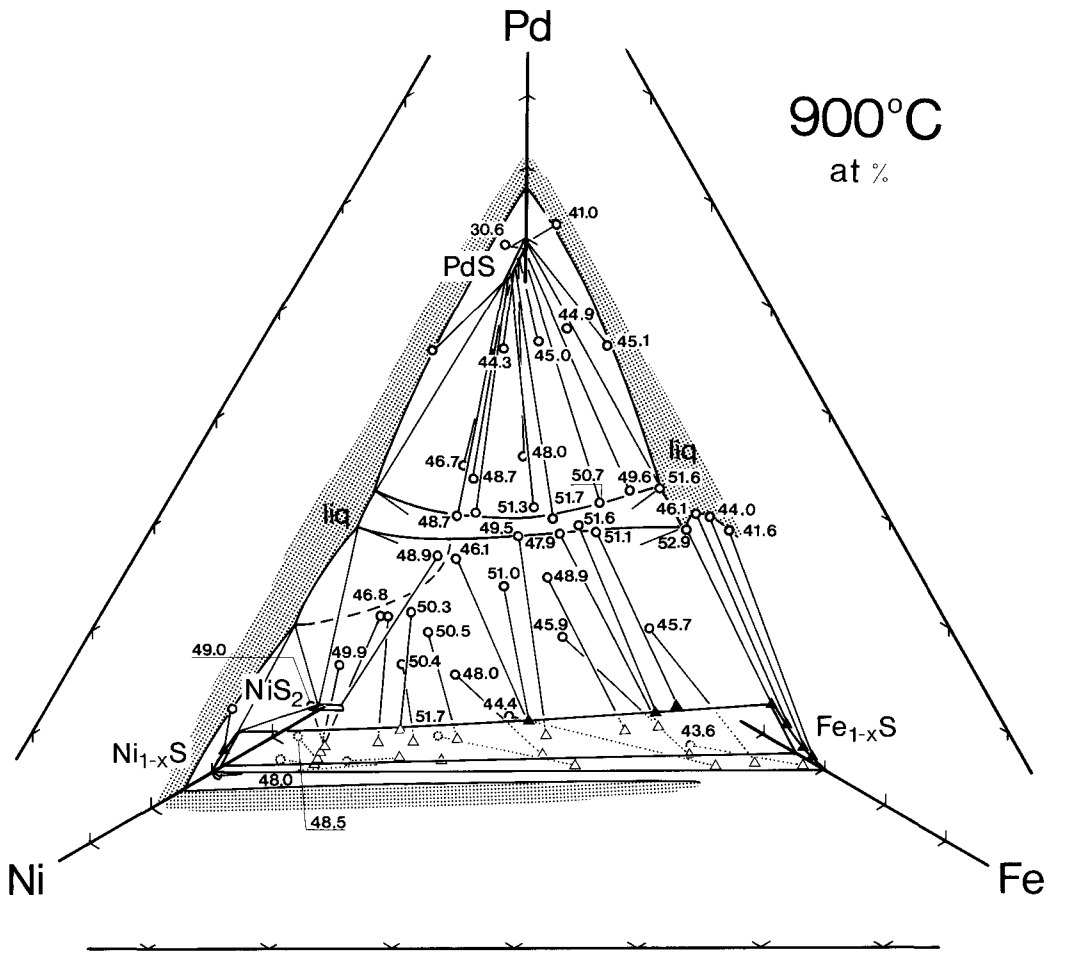

FIG. 5. Parallel projection, onto the Pd–Ni–Fe plane, of assemblages involving the upper, S-rich surface of the sulphide melt volume in the system Pd–Fe–Ni–S at 900°C. The ternary 'walls' of the melt volume are stippled; melt compositions are indicated by circles (at.% S in the melt are given), *mss* compositions $(Fe,Ni)_{1-x}S$ by triangles.

presence of vaesite, NiS_2 (Kullerud, 1963). Our results indicate solubility of 2.0 at.% (2.7 wt.%) Fe and 1.0 at.% (2.6 wt.%) Pd at this temperature. This composition is associated with *mss* and sulphide melt which contains 20.3 at.% (39.6 wt.%) Pd; Fe/(Fe+Ni) = 0.27 (0.26 by weight).

Phase relations at 725°C

Boundary systems. In the boundary system Pd-Ni-S (Karup-Møller and Makovicky, 1993) the sulphide liquid spans the entire spectrum of Ni/Pd ratios as does the γ-(Ni,Pd) alloy. Phase relations are complicated by the appearance of $Ni_{3\pm x}S_2$ with appreciable solubility of Pd (2.0 at.%; 4.4 wt.%). The sulphide melt–sulphur binary field disappears, so that Ni sulphides and PdS can coexist in the three-phase fields $Ni_{1-x}S$–PdS–melt and $Ni_{1-x}S$–PdS–NiS_2.

In the boundary system Pd–Fe–S (Makovicky and Karup-Møller, 1993) the sulphide liquid receded to Pd-enriched compositions, beyond the Pd/Fe ratio of 3:2 (74:26 by weight). At lower S contents the phase relationships are dominated by the three-phase assemblages FeS–α-Fe–γ-(Fe,Pd) and pyrrhotite (0.1 at.% Pd)–Pd_3Fe–melt. At high sulphur contents, assemblages analogous to those in the Pd–Ni–S system develop.

Because of the discrepancies between our results and the interpolated data of Kullerud *et al.* (1969) and Craig and Kullerud (1969) for 850 and 650°C,

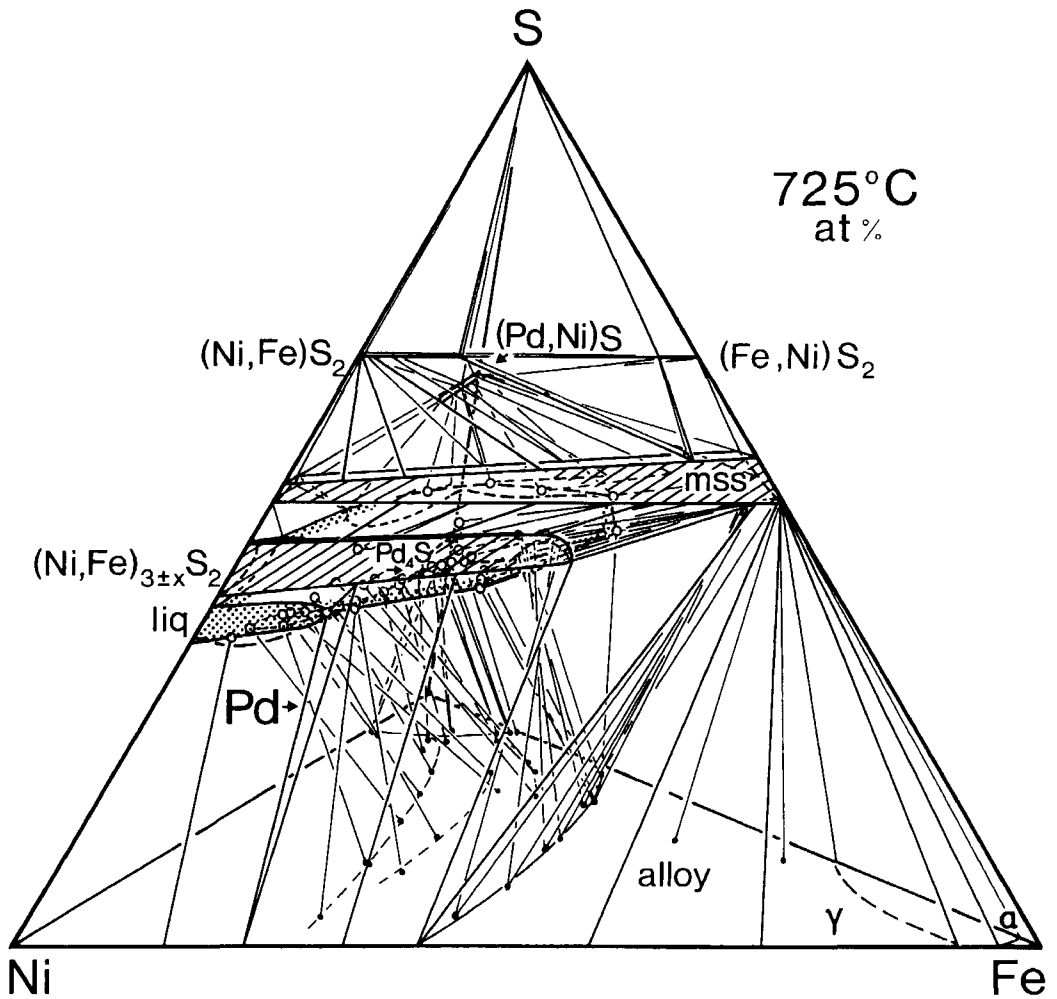

FIG. 6. Principal features of the system Pd–Fe–Ni–S at 725°C. Sulphide melt is stippled, single-phase fields in the system Ni–Fe–S are ruled. Selected tie-lines are shown.

we have studied the Ni–Fe–S system at 725°C in detail (Karup-Møller and Makovicky, in press). Our results indicate that the Ni–Fe–S melt extends from the Ni–S join to 11.9 at.% (13.6 wt.%) Fe. The high-temperature phase $(Ni,Fe)_{3\pm x}S_2$ extends far from the Ni–S join and reaches ~32.6 at.% (~39.4 wt.%) Fe. On quenching it does not survive and alters to $(Ni,Fe)_3S_2$ for low Fe contents, and via complex mixtures, to pentlandite + alloy at high iron contents. NiS_2 dissolves about 10 at.% (13.7 wt.%) Fe, whereas FeS_2 only 3.4 at.% (5.0 wt.%) Ni.

Comparably to the situation at 900°C, high solubility of Ni in PdS (8.2 at.%; 7.4 wt.%) contrasts with the low solubility of Fe in this phase (0.4 at.%; 0.3 wt.%). Solubility of Pd in $Fe_{1-x}S$ and $Ni_{1-x}S$ behaves in the opposite way (2.0 at.%; 4.8 wt.% and 1.1 at.%; 2.6 wt.%, respectively).

Alloy-containing associations in the quaternary system Pd–Fe–Ni–S. The low-sulphur area of the quaternary phase system at 725°C was investigated using the same charge strategy as for 900°C, with additional charges in the areas with complex phase relations.

At 725°C an immiscibility gap exists between α-Fe with low solubility for Ni and Pd and the γ-(Ni,Fe,Pd) alloy (Moffatt, 1984). Its shape, in equilibrium with *po*, could be mapped out only approximately (Fig. 6). The density of our charges did not yield any

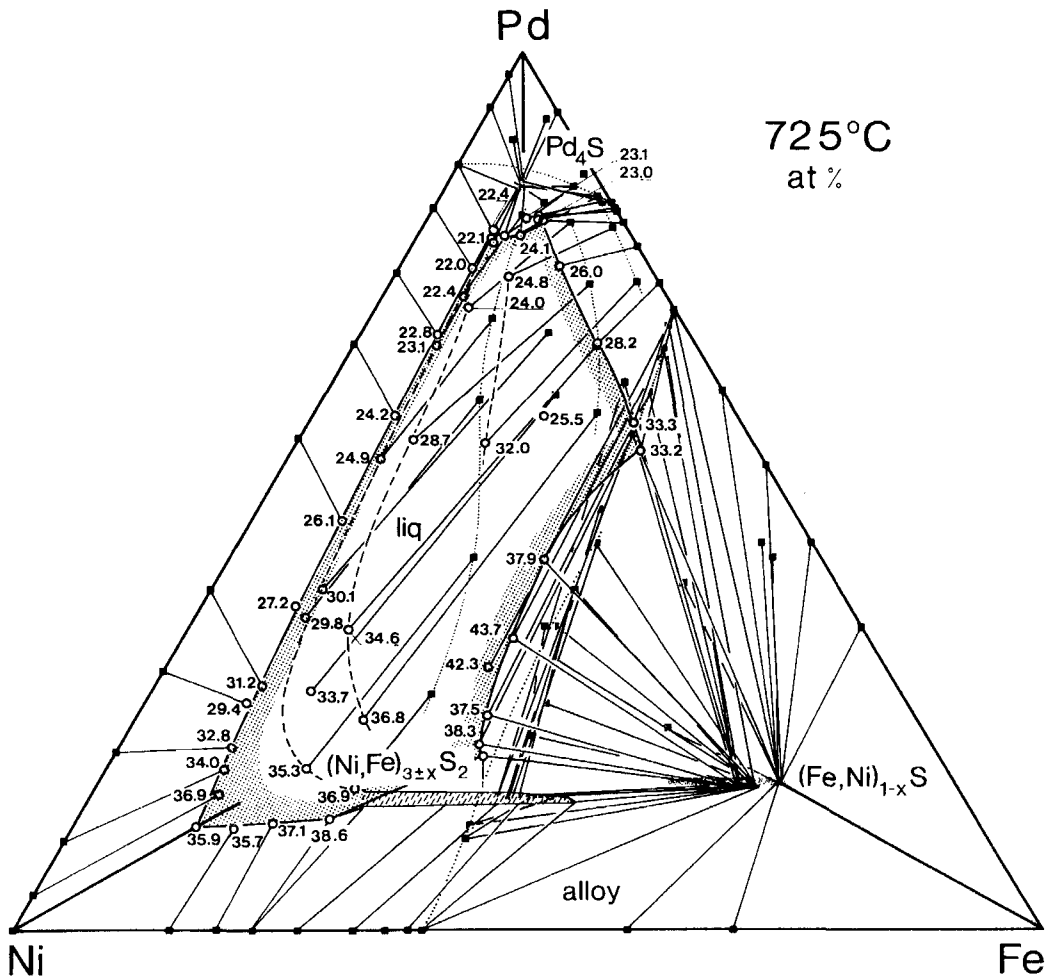

FIG. 7. Parallel projection of alloy-containing associations in the system Pd–Ni–Fe–S at 725°C onto the Pd–Fe–Ni plane. Conventions as in Fig. 3.

information on the behaviour of Fe–Pd ordering in the alloys with increasing Ni contents. With secondary alloy present in all quenched melts from these portions of the system, X-ray diffraction of melt–alloy charges was clearly irrelevant.

The sulphide melt shrank to Pd–Ni-enriched areas of the quaternary composition space, between the Pd–Ni join and the points (25 at.% Fe, ~40 at.% Pd, ~35 at.% S; 20.6 wt.% Fe, 62.8 wt.% Pd and 16.6 wt.% S) and ~ (50.6 at.% Ni, 11.9 at.% Fe and 37.5 at.% S; 60.7 wt.% Ni, 13.6 wt.% Fe and 24.6 wt.% S). The alloy–melt tie-lines are remarkably similar to those at 900°C, both in their direction and length (i.e. enrichment factors; Fig. 7). The same variations as at 900°C take place in the Pd enrichment of alloy over the coexisting melt along the range from 0 to 100% Pd. Again, the S-poor surface of the melt field moves to lower S contents with increasing Pd contents (Fig. 7).

Pyrrhotite with low S contents forms two-phase associations with α-Fe and γ-(Fe,Pd) and three-phase associations *po*–$(Ni,Fe)_{3\pm x}S_2$–alloy and *po*–melt–alloy, as illustrated in Figs. 7 and 8. For the latter association, increase in the Ni/Pd ratio for the alloy and the melt is accompanied by an increase in the Ni/Fe ratio of pyrrhotite. The alloy compositions that partake in various two-phase and three-phase associations are shown in Fig. 9, whereas the element distributions for the alloy–melt pairs are shown in Fig. 10.

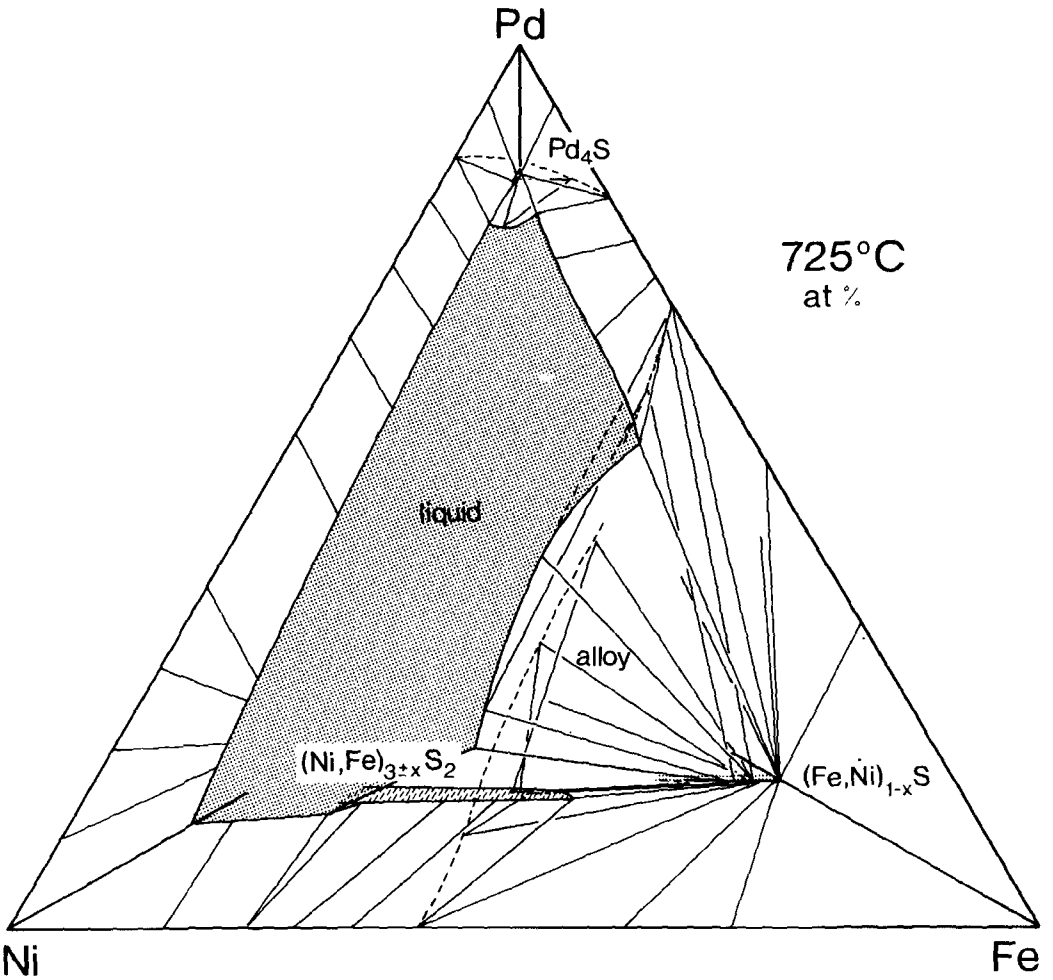

FIG. 8. A simplified vertical projection of the alloy-containing assemblages of the system Pd–Ni–Fe–S at 725°C. Dashed curves indicate traces of three-phase assemblages in the composition plane of Pd–Fe–Ni alloys.

Alloy-free sulphide associations in the quaternary system Pd–Fe–Ni–S. At 725°C the upper portion of the tetrahedron Fe–Ni–Pd–S is dominated by the ternary assemblage *mss*–(Ni,Fe)S_2–(*Pd*,Ni)S (Fig. 11a). The disulphide phase forms a continuous solid solution, NiS_2–(*Ni*,Fe)S_2 with the maximum Fe contents reaching 10 at.% (13.5 wt.%) Fe. It has a geologically important solubility of Pd, which is below 0.5 at.% (1.3 wt.%) in NiS_2 but reaches 1–1.4 at.% (2.6–3.6 wt.%) for moderate to maximum Fe contents.

The successive levels of this ternary assemblage involve more and more Ni-enriched portions of all three solid solutions (Fig. 11*a*). Nickel increments are largest on $(Fe,Ni)_{1-x}S$ (with Pd contents between 1 and 2 at.% (2.4–4.8 wt.%) Pd, i.e. the highest Pd contents for *mss* at this temperature), intermediate on the disulphide solid solution and smallest on (Pd,Ni,Fe)S. This assemblage represents, at 900 and 725°C, the first instance of a measurable primary Pd content in an important base-metal disulphide, $(Ni,Fe)S_2$, found in our synthetic runs. Our present results are comparable to the results obtained on CoS_2 at 1000–800°C (Karup-Møller and Makovicky, 1986), but the values for dissolved Pd are twice those of CoS_2.

The solubility of Ni in FeS_2 is moderate at 725°C, with a measured maximum of 3.4 at.% (4.6 wt.%). Along its short solid solution field, FeS_2 dissolves only uncertain traces of Pd; maximum measured Pd

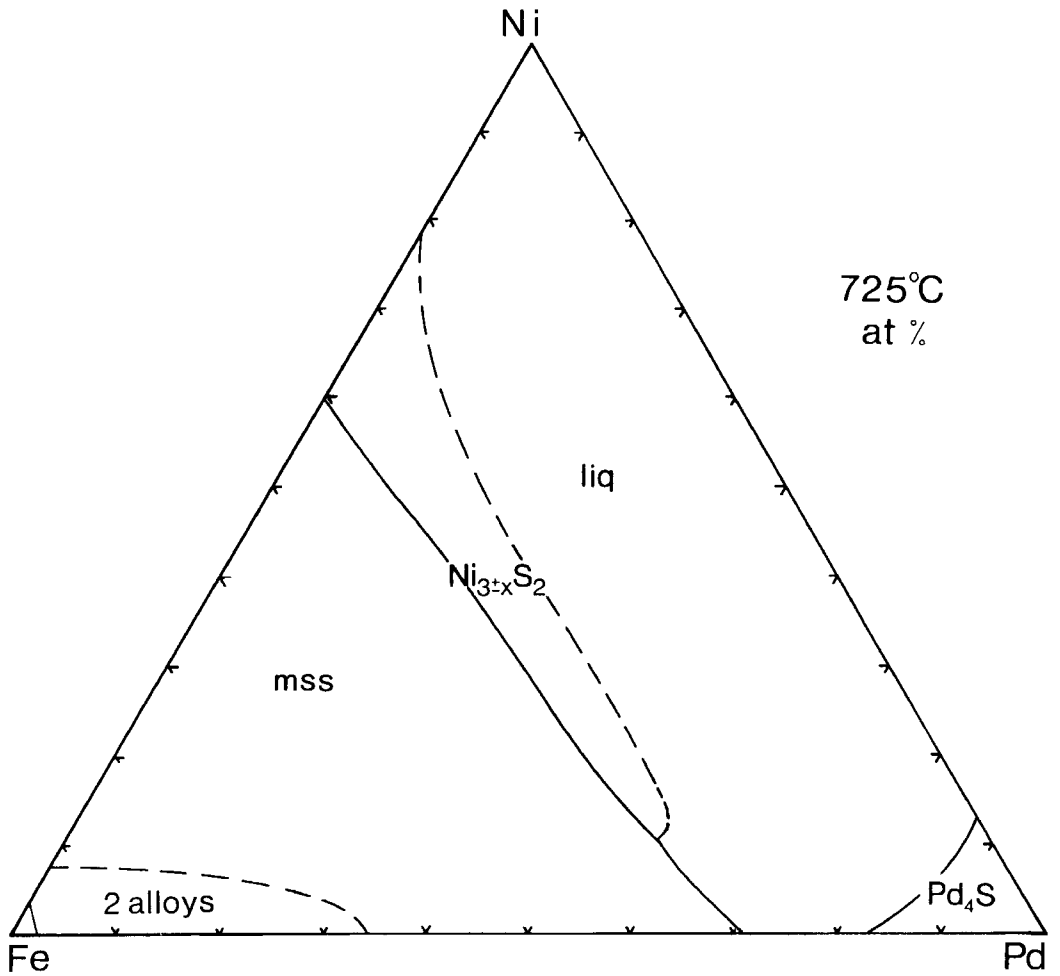

FIG. 9. Alloy compositions partaking in various phase assemblages of the Pd–Ni–Fe–S system at 725°C.

contents were 0.1 % at (0.3 wt.%). FeS_2 coexists with *mss* and PdS that are poor in Ni (Fig. 11*a*). The quaternary assemblage vaesite–pyrite–PdS–*mss* is characterized by the following compositions: $(Ni,Fe)S_2$ contains 9.0 at.% (12.2 wt.%) Fe and 1.0 at.% (2.6 wt.%) Pd; FeS_2 contains 3.4 at.% (4.6 wt.%) Ni and <0.1 at.% (0.2 wt.%) Pd; PdS contains 1.1 at.% (0.9 wt.%) Ni and 0.1 at.% (0.1 wt.%) Fe; and *mss* contains 6.3 at.% (8.4 wt.%) Ni, 2.0 at.% (4.8 wt.%) Pd and 54.9 at.% (40.0 wt.%) S. In the Pd-free run, for the analogous three-phase assemblage, *mss* contains 6.7 at.% (9.7 wt.%) Ni, whereas FeS_2 3.6 at.% (4.9 wt.%) Ni. In the vaesite–pyrite–PdS–*mss* assemblage, the Ni contents in PdS are slightly lower than those for the analogous disulphide-free assemblage *mss*–PdS, in full agreement with the lower solubility of Ni in PdS at higher sulphur fugacities, found in the phase system Pd–Ni–S by Karup-Møller and Makovicky (1993). The most S-rich part of the system Pd–Fe–Ni–S contains the association of the two disulphides with S and PdS (with 1.2 at.% (1.0 wt.%) Ni).

The question of Pd solubility in FeS_2 at 725°C should not be confused with the occurrence of PGE in pyrite in the form of PGM exsolutions that represent relics of exsolutions from pyrrhotite which was later sulphidized into pyrite during low-temperature annealing. Such a case was described for Pt in synthetic runs in the system Fe–Pt–S by Makovicky *et al.* (1988).

In the phase assemblage *mss*–PdS the S contents and Pd contents of *mss* are below those of the

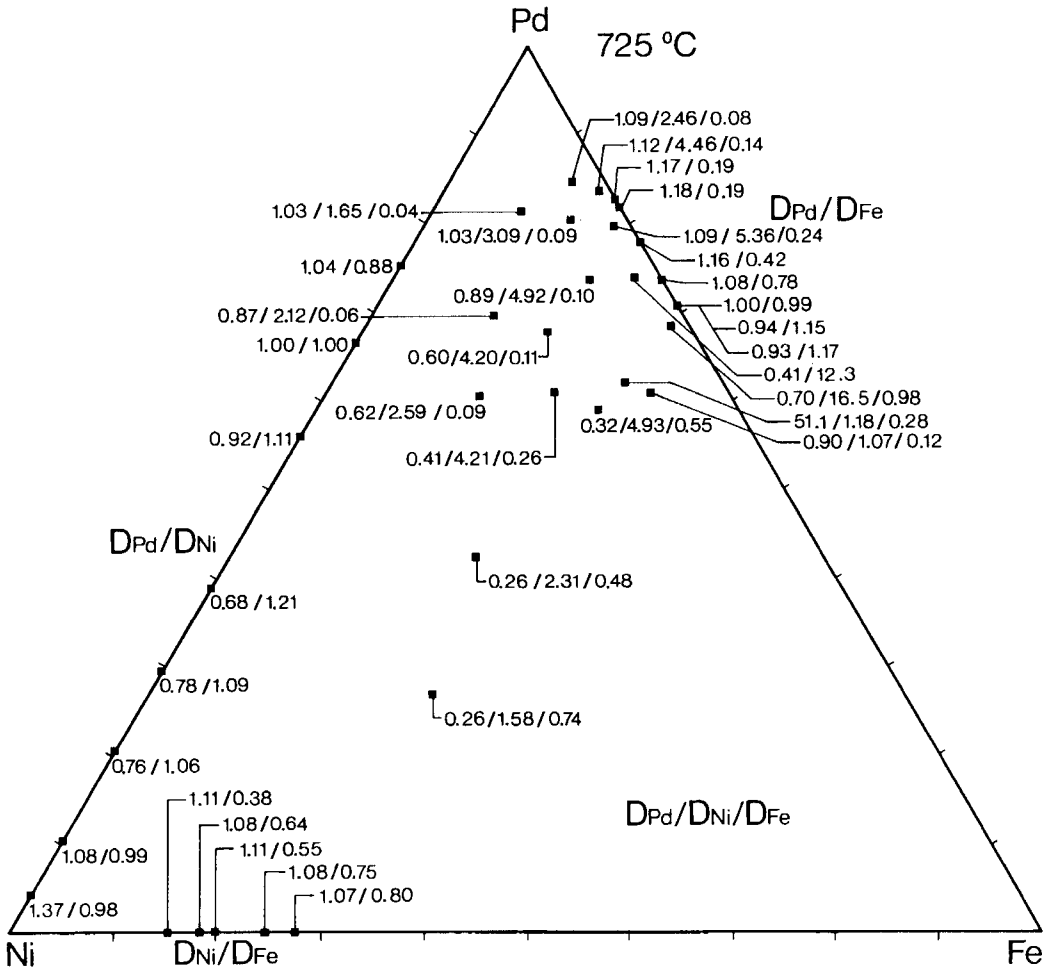

FIG. 10. Distribution coefficients melt/alloy for Pd, Ni, and Fe at 725°C, inscribed at the appropriate alloy compositions.

assemblages just considered (Fig. 11*b*). The Ni/Pd ratio in PdS reaches its highest value in this assemblage and changes linearly with the Ni/Fe ratio in *mss*. Fe contents in PdS are below 0.5 at.% (<0.4 wt.%). For pure $Ni_{1-x}S$, PdS contains 8.2 at.% (7.4 wt.%) Ni and for 33.7 at.% (43.9 wt.%) Ni in *mss* there is 5.7 at.% (5.0 wt.%) Ni in PdS; in the regions poorer in Ni these respective values are 22.4 and 4.1 at.% (29.3 and 3.6 wt.%) Ni, and 8.2 and 1.4 at.% (10.8 and 1.2 wt.%) Ni. The density of data is too low to describe exactly the variation of Ni/Pd ratio in PdS with the varying S content in associated *mss* with a constant Ni/Fe ratio. In the Ni-rich and moderate-Ni portions of the (Pd,Ni)S solid solution the Ni/Pd ratio appears to increase with decreasing sulphur fugacity.

In the adjacent assemblage *mss*–PdS–melt (Fig. 12) the tie-lines *mss*–PdS preserve the orientation of tie-lines from the assemblage PdS–*mss*. Sulphide–melt compositions for the eutectic co-crystallization of PdS and *mss* at 725°C connect melts richer in Pd ($Fe_{20}Pd_{32.5}S_{47.5}$, i.e. 18.3 wt.% Fe, 56.7 wt.% Pd and 25.0 wt.% S) on the iron side of the composition space with melts poorer in Pd ($Ni_{34}Pd_{22}S_{44}$, i.e. 34.7 wt.% Ni, 40.7 wt.% Pd and 24.5 wt.% S) on the Ni side of this space (Fig. 12). For the ratio Ni/Fe = 1.925 (2.024 by weight) in *mss* (and 5.6 at.% (4.9 wt.%) Ni in PdS) the eutectic melt has the metal ratio $Ni_{42.3}Fe_{14.2}Pd_{43.5}$ (31.4:1.0:58.6 by weight). For Ni/Fe = 0.551 (0.579 by weight) in *mss* (3.5 at.% (3.0 wt.%) Ni in PdS) this ratio represents $Ni_{25.7}Fe_{22.9}Pd_{51.4}$ (18.3:15.5:66.2 by

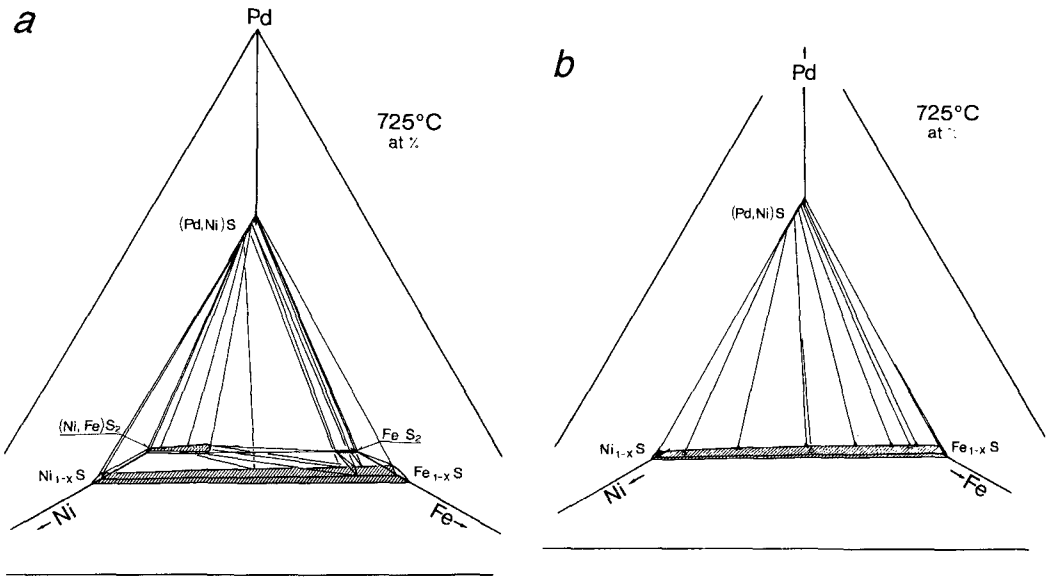

FIG. 11. The S-rich portion of the system Pd–Fe–Ni–S at 725°C in parallel projection onto the Pd–Ni–Fe plane: (*a*) the monosulphide–disulphides–PdS assemblage; (*b*) the PdS–$(Fe,Ni)_{1-x}S$ assemblage. Only the *mss* portions involved in these phase assemblages are plotted.

weight), and for Ni/Fe = 0.184 (0.193 by weight) in *mss* (1.8 at.% (1.5 wt.%) Ni in PdS) the metal ratio in the melt is $Ni_{12.7}Fe_{27.8}Pd_{59.5}$ (8.6:18.0:73.4 by weight).

The Me/S ratio in the eutectic melt is very constant, about $Me_{60\text{-}59}S_{40\text{-}41}$, except for the Ni-rich quarter of the system where the sulphur content rises to 42–43 at%. With the exception of the most Fe-rich region, the eutectic melt is moderately enriched in Ni in comparison with the associated tie-line (i.e. with the weighted mean for *mss*–PdS). Pd contents of *mss* in this assemblage are quite uniform along the entire Ni/Fe spectrum of compositions, from 1.6 at.% (3.8 wt.%) Pd at the Fe end to 1.1 at.% (2.6 wt.%) Pd at the Ni end.

Rather important volumes of the composition space Pd–Ni–Fe–S are occupied by the binary assemblages PdS–sulphide melt and *mss*–sulphide melt. In the first assemblage the Ni/Pd ratio in PdS appears to be a function of the Ni/Fe ratio in the melt; according to rather limited data, the Pd content of the melt exercises comparatively little influence (Fig. 12).

The situation is completely different for the association *mss*–melt. As found at 900°C, the S content of the $(Fe,Ni,Pd)_{1-x}S$ solid solution (=*mss*) is intimately related to the Ni/Fe and Pd/ΣMe ratios in the melt. For near-stoichiometric (Fe,Ni)S with up to 0.15 at.% (0.4 wt.%) Pd, the melt is highly enriched in Ni, especially for the Fe-rich *mss* compositions. This melt regularly contains ~ 7 to 8 at.% (14.5–16 wt.%) Pd and this association always involves $(Ni,Fe)_{3\pm x}S_2$ that dissolves ~1.5 at.% (3.5 wt.%) Pd. As the S contents in *mss* rise above ~51 at.% (~37.4 wt.%), the tie-lines of the binary assemblage *mss*–melt rotate clockwise and reach to higher and higher Pd contents in the melt until they reach the eutectic curve. For this association their deviation from the respective tie-lines *mss*–PdS is small.

Remarkably, for any individual Ni/Fe ratio in *mss* the S contents of associated melts show little change, below the accuracy of the analyses. It means that the S-rich surface of the melt volume in the composition space Pd–Fe–Ni–S is rather flat all over the Pd-poor portion, in spite of the substantial change in the S contents of the associated *mss*, i.e. in sulphur fugacity. It starts dipping considerably towards metal-rich compositions in the association PdS–melt, for Pd contents higher than those on the cotectic. The melt volume has receded considerably in comparison to that at 900°C, away from the Fe-rich compositions, so that the tie-lines between Fe-rich *mss* and melt become especially long (Fig. 12).

Assemblages that involve Pd-poor melt, *mss* and $(Ni,Fe)_{3\pm x}S_2$ are very difficult to unravel from the textural point of view. For example, melt compositions are removed by only a few atomic percent from the composition field of coexisting $(Ni,Fe)_{3\pm x}S_2$

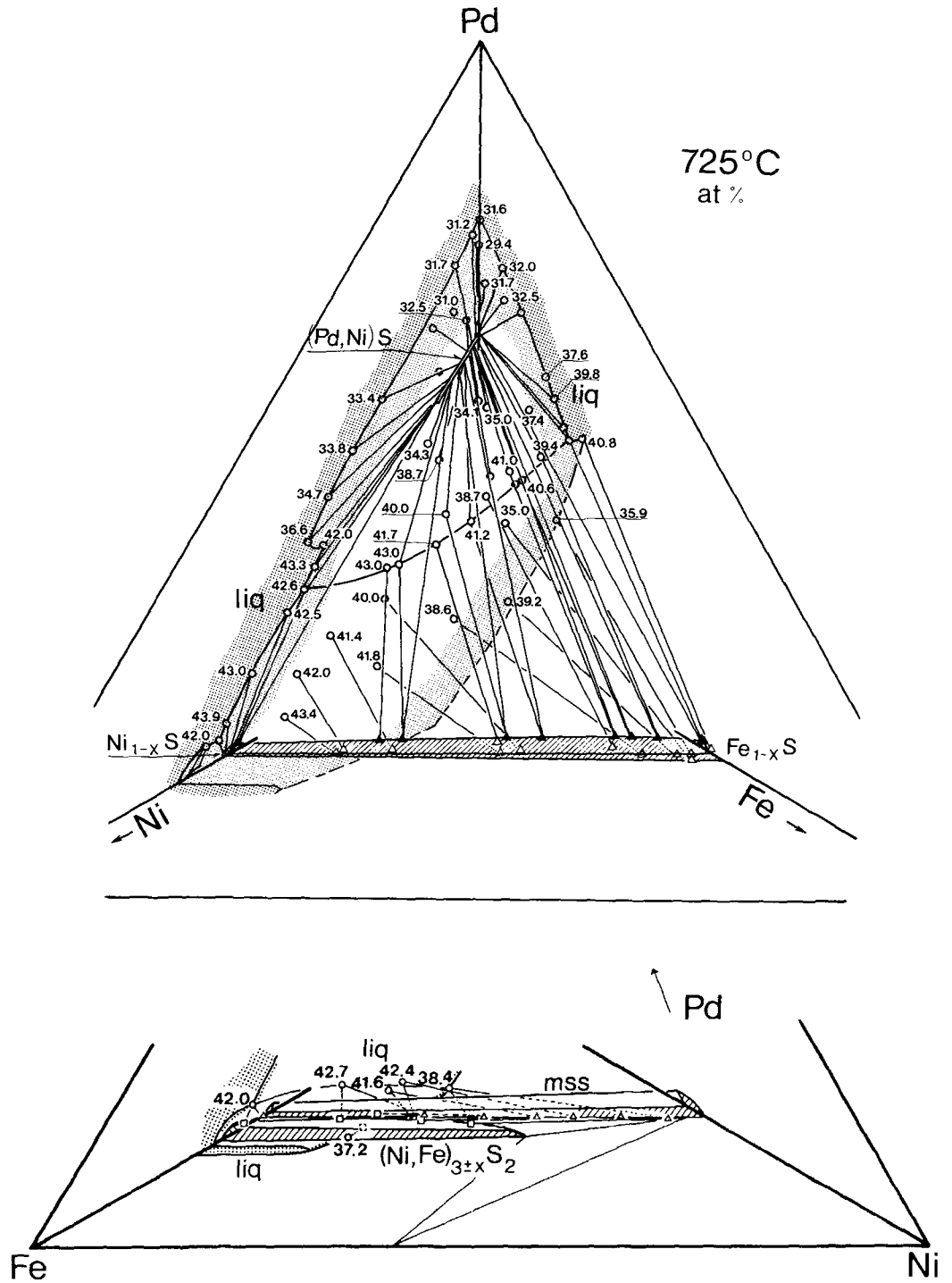

FIG. 12. Parallel projection, onto the Pd–Ni–Fe plane, of the phase assemblages involving sulphide melt, $(Fe,Ni)_{1-x}S$ and PdS. Inset: details of phase assemblages that involve $(Ni,Fe)_{3\pm x}S_2$. Conventions as in Fig. 5.

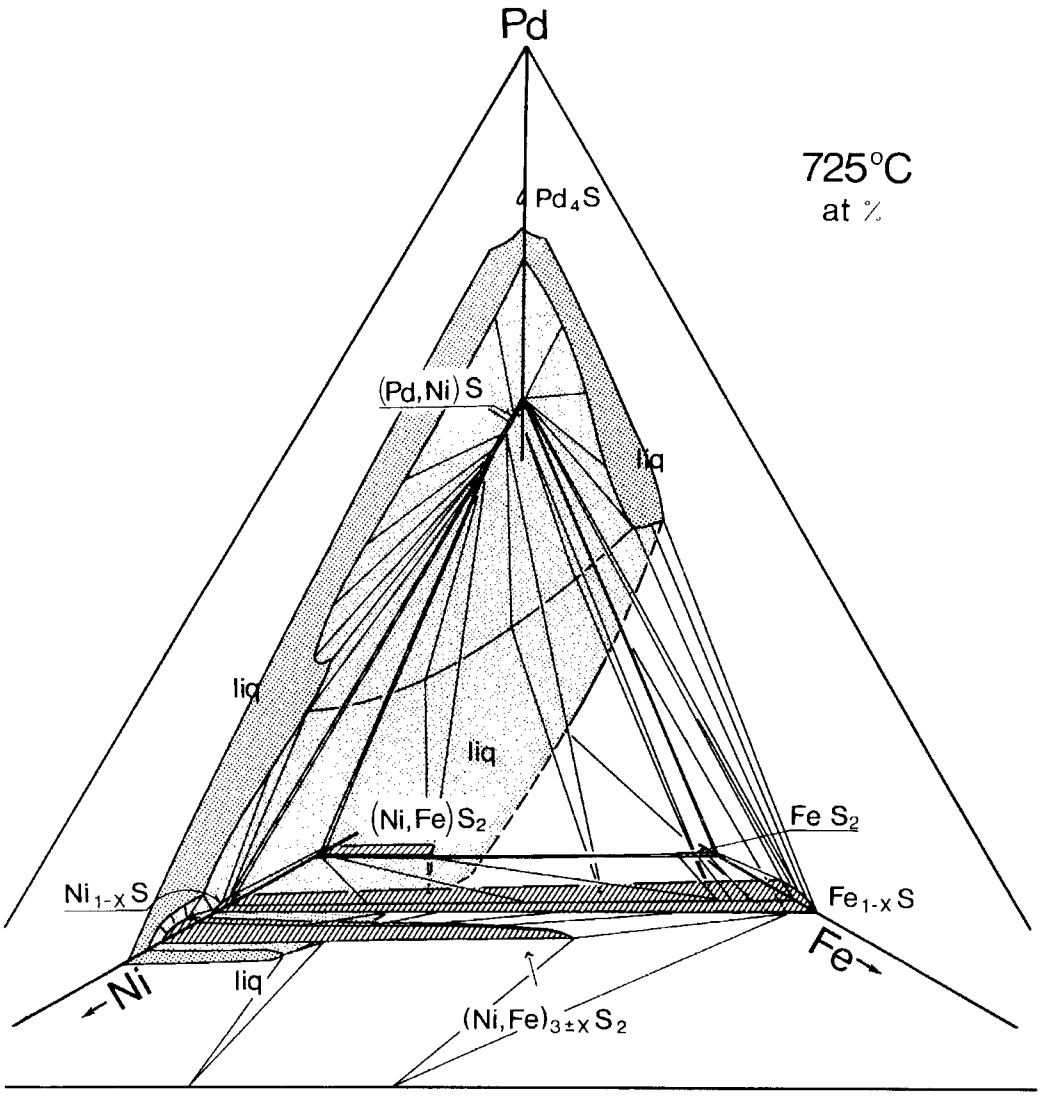

FIG. 13. Top view (parallel projection from the S apex) of the alloy-free assemblages in the system Pd–Ni–Fe–S. Fields of solid phases are hatched, that of the sulphide melt is stippled. Selected tie-lines are indicated.

(Fig. 13). When this melt solidifies on quenching, it represents an aggregate of $(Ni,Fe)_{3\pm x}S_2$ crystals with just a few percent of other interstitial phases – PdS, *mss* or pentlandite. The high-temperature polymorph of $Ni_{3\pm x}S_2$ is non-quenchable and decomposes into Ni_3S_2, mixed with another phase(s) (Kullerud and Yund, 1962). This happens both in the original, pure, Pd-bearing $(Ni,Fe)_{3\pm x}S_2$ phase and in crystals of this phase which form from the melt on quenching, making the resulting texture exceedingly complex. Pentlandite is a common product obtained on quenching of the Fe-rich portions of $(Ni,Fe)_{3\pm x}S_2$ (in agreement with Kullerud, 1963), together with a finely dispersed alloy that forms during quenching from the difference in metal contents between $(Ni,Fe)_{3\pm x}S_2$ and $(Ni,Fe)_9S_8$ (Misra and Fleet, 1973; Karup-Møller and Makovicky, in press).

Recently, Kitakaze and Sukagi (1992) and Sugaki and Kitakaze (1992) described a non-quenchable low-to-high phase transition in pentlandite, $Fe_{4.5}Ni_{4.5}S_9$, at 610°C during which the 10.1 Å cubic cell of pentlandite changes into an F-centred

5.3 Å cubic cell. The high form is stable up to 829°C, with compositions given as $Fe_{3.62}Ni_{5.68}S_{7.70}$ for 770°C and $Fe_{4.5}Ni_{4.5}S_{7.99}$ for 800°C. In the series $Fe_{4.5}Ni_{4.5}S_8$–Co_9S_8 the high form and the low form should coexist over a temperature range of as much as 40°C.

Unlike the Japanese authors, we interpret the high-temperature phase as a part of the broad solid solution field $(Ni,Fe)_{3\pm x}S_2$. Its compositions between Fe:Ni = 1:1 and the pure Ni charges that we investigated were not examined by the Japanese authors. The 5 Å F-centred cubic unit cell was found for high-temperature $Ni_{3\pm x}S_2$ by Liné and Huber (1963); for the stoichiometric Ni_3S_2 the unit-cell parameter is 5.2 Å at 640°C.

For the most Pd-poor and Pd-free portions of the studied compositional space, the binary assemblage $(Ni,Fe)_{3\pm x}S_2$–*mss* gains importance; the above phenomenon of decompostion on quenching plagues this portion as well. $(Ni,Fe)_{3\pm x}S_2$ can contain up to 32.6 at.% (39.4 wt.%) Fe and is associated in this case with Fe-rich *mss* (2.6 at.% (3.4 wt.%) Ni). For this case, $(Ni,Fe)_{3\pm x}S_2$ has the Ni/Fe ratio equal to 0.73, whereas in *mss* this ratio is 0.05; for two other typical charges these ratios are 5.63 (resp. 2.20) for $(Ni,Fe)_{3\pm x}S_2$ and 2.89 (resp. 0.73) for *mss* (Fig. 13).

Conclusions

(1) At 900 and 725°C, phase assemblages involving sulphide melt dominate the compositional space Pd–Ni–Fe–S (except for its most S-rich portions at 725°C). Even at 900°C the melt does not reach the Fe-rich portions of the system (but does at 988°C; Kullerud, 1967). Its retreat away from Fe-rich compositions between 900 and 725°C (continuing towards 550°C) is fast. Melt compositions coexisting with *mss* alter substantially as the temperature decreases.

(2) The field of *mss* is uninterrupted at both 900 and 725°C. For the association *mss*–S–melt, resp. $(Ni,Fe)_{1-x}S$–$(Ni,Fe)S_2$–melt, maximum Pd solubilities in *mss* (given below for the Fe- and Ni-rich ends of *mss*, respectively) are 5.5 at.% (12.8 wt.%) and 2.1 at.% (4.9 wt.%) at 900°C. For the association *mss*–PdS–disulphide(s), maximum Pd solubilities in *mss* are 2.0 at.% (4.8 wt.%) and 1.1 at.% (2.6 wt.%); they occur at 725°C. For *mss*–PdS–melt, they are 1.6 at.% (3.8 wt.%) and 1.1 at.% (2.6 wt.%), again at 725°C. For the association melt–alloy–*mss*, the solubility of Pd in Fe-rich *mss* was found to be ~0.13 at.% (0.3 wt.%) Pd at 900°C and 0.17 at.% (0.4 wt.%) Pd at 725°C.

(3) For the majority of bulk compositions, and at all temperatures, the sulphide melt is strongly enriched in Ni and impoverished in Pd in comparison to the associated alloy. Both melt and alloy have similar proportions of Fe. The situation is altered for Pd-rich melts and in the regions close to the bounding systems Ni–Pd–S and Ni–Fe–S. Numerical Ni, Pd and Fe distribution coefficients alloy/melt were mapped out for the entire melt region at both 900 and 725°C.

(4) For the most Pd-poor compositions, the sulphide melt in association with S-poor *mss* (± $Ni_{3\pm x}S_2$ at 725°C) is strongly enriched in Ni with respect to *mss*. With rising sulphur contents in *mss* the tie-lines *mss*–melt rotate clockwise and at both examined temperatures lead to melts progressively richer in Pd that have the Ni/Fe ratios closer and closer to that of *mss* (or close to the *mss*–PdS tie-lines at 725°C). Distribution coefficients *mss*/melt are derived (Makovicky *et al.*, 1994) and will be discussed elsewhere (Barnes *et al.*, in prep.).

(5) At 725°C, many bulk compositions in the more S-rich part of the system will lead to the association $(Ni,Fe)S_2$–PdS–*mss*. Nickel contents in these three solid solutions rise or fall concurrently. Adding Ni-bearing FeS_2 to this assemblage leads to Ni-poor *mss* and PdS as associated phases.

(6) At 900°C *mss* and PdS cannot co-crystallize, their fields being separated by a binary assemblage sulphide melt–sulphur. At 725°C they co-crystallize for all Ni/Fe ratios in the assemblages *mss*–PdS–disulphide(s), *mss*–PdS and *mss*–PdS–melt.

(7) The quasi-linear solid solutions (Pd,Ni)S and Fe-rich *mss* participate in a number of binary and ternary assemblages in which they have similar Ni/Pd and Ni/Fe ratios. The principal compositional difference from one such assemblage to another is the change in the Me/S ratios of PdS and *mss*. In the case of PdS this change will be almost imperceptible by electron microprobe analysis and nearly so for *mss* in alloy-containing assemblages. In PdS these variations are connected with a small change in Fe/ΣMe, in *mss* with a marginal change in the Pd/ΣMe ratio.

(8) Our quantitative data allow (*a*) the estimation of compositions and fractionation of original sulphide melt associated with alloys present in deposit; (*b*) the same for the S-rich melts by examining the *bulk* compositions of Pd-bearing pyrrhotite (i.e. including the exsolved particles); (*c*) the estimation of S-rich melt compositions by examining the composition of Ni-bearing braggite (for the temperature dependence, see Karup-Møller and Makovicky, 1993). The data may also be used to estimate the Pd-bearing/concentrating potential of alloys, pyrrhotite, $(Ni,Fe)S_2$, $Pd_{2.2}S$ (vasilite, Atanosov, 1990; Augé and Legendre, 1992), Pd_4S (recently discovered as a mineral, Augé and Legendre, 1992), and the high-temperature $Ni_{3\pm x}S_2$.

Further conclusions can be drawn after the 550 and 400°C data have been fully processed and prepared for publication. The main obstacles to the geological interpretation of the presented high-temperature data are the problems of 'subtraction' of the overprint by later, often extensive, subsolidus reactions in the PGE deposits.

Acknowledgements

This project represents a part of the European Community project 'Factors governing concentrations of PGE in layered complexes' (contract No. M1AM-006-DK(B) of the EEC Primary Raw Materials and Recycling Programme). We are deeply grateful to the EEC for the principal financial support. Contributions of the University of Copenhagen and the financing of the microprobe laboratory by the Danish Natural Science Research Council are gratefully acknowledged as well. Dr C.K. Brooks and an unknown reviewer kindly helped to improve the quality of the manuscript. Kind assistance and interest of Mr. Sinh Hy, lecturer J.G. Rønsbo, Mr J. Fløng, Mrs M.L. Johansen, and Mrs B. Holm, and of our colleagues in the above EEC project were greatly appreciated.

References

Arnold, R.G. and Malik, O.P. (1975) The NiS–S system above 980°C — a revision. *Econ. Geol.*, **70**, 176–82.

Atanosov, A.V. (1990) Vasilite, $(Pd,Cu)_{16}(S,Te)_7$, a new mineral species from Novoseltsi, Bulgaria. *Canad. Mineral.*, **28**, 687–9.

Augé, T. and Legendre, O. (1992) Pt–Fe nuggets from alluvial deposits in eastern Madagascar. *Canad. Mineral.*, **30**, 983–1004.

Barnes, S.-J., Makovicky E., Karup-Møller, S., Makovicky, M. and Rose-Hansen J. (1994) Partition coefficients for Ni, Cu, Pd, Pt, Rh and Ir between mono-sulphide solid solution and sulphide liquid and the implications for the formation of compositionally zoned Ni–Cu sulphide bodies by fractional crystallization of sulphide liquid. *Mineral. Mag.*, **58A**, 51–2.

Bryukvin, V.A., Shekhter, L.N., Reznichenko, V.A., Kuvinov, V.E., Blokhina, L.I. and Kukoyev, V.A. (1985) Phase equilibria in the system Fe–Pd–S (in Russian). *Izv. AN SSSR Metally*, **4**, 25–8.

Clark, L.A. and Kullerud, G. (1963) The sulfur-rich portion of the Fe–Ni–S system. *Econ. Geol.*, **58**, 853–85.

Craig, J.R. and Kullerud, G. (1969) Phase relations in the Cu–Fe–Ni–S system and their application to magmatic ore deposits. In *Magmatic Ore Deposits* (H.D.B. Wilson, ed.). *Econ. Geol Monograph*, **4**, 344–58.

Distler, V.V. (1980) Solid solutions of platinoids in sulphides (in Russian). In *Sulphosalts, plattinum minerals and ore microscopy*. Proc. General Meeting IMA, Novosibirsk 1978. IGEM AN SSSR, Nauka, 191–200.

Distler, V.V., Malevsky, A.Y. and Laputina, I.P. (1977) Distribution of platinoids between pyrrhotite and pentlandite during the crystallization of sulphide melt (in Russian), *Geokhimiya*, **11**, 1646–57.

Elliot, R.P. (1965) *Constitution of binary alloys*, 1st supp.: New York, McGraw-Hill Book Co., 877 pp.

Hansen, M. and Anderko, K. (1958) *Constitution of binary alloys*, 2nd ed.: New York, McGraw-Hill Book Co., 1305 pp.

Karup-Møller, S. and Makovicky, E. (1986) The system Pd–Co–S at 1,000°, 800°, 600°, and 400°C. *Econ. Geol.*, **81**, 1049–55.

Karup-Møller, S. and Makovicky, E. (1993) The system Pd–Ni–S at 900°, 725°, 550°, and 400°C. *Econ. Geol.*, **88**, 1261–8.

Karup-Møller, S. and Makovicky, E. (in press) The phase system Fe–Ni–S at 725°C. *Neues Jahrb. Mineral. Mh.*

Kitakaze, A. and Sugaki, A. (1992) Phase transition of pentlandite–cobalt pentlandite series and its phase relations: *Abstr. 29th Internat. Geol. Congr. Kyoto* **3**, 678.

Kullerud, G. (1963) The Fe–Ni–S system. *Carnegie Inst. Wash. Year Book*, **62**, 175–89.

Kullerud, G. (1967) Sulfide studies. In: *Researches in Geochemistry*. (P.M. Abelson, ed.), New York, John Wiley and Sons 2, 286-321.

Kullerud, G. and Yund, R.A. (1962) The Ni–S system and related minerals. *J. Petrol.*, **3**, 126–75.

Kullerud, G., Yund, R.A. and Moh, G.H. (1969) Phase relations in the Cu–Fe–S, Cu–Ni–S, and Fe–Ni–S systems. In: *Econ. Geol. Monograph*, **4** (H.D.B. Wilson, ed.) 323–43.

Liné, G. and Huber, M. (1963) Etude radiocristallographique à haute temperature de Ia phase non-stoechiométrique $Ni_{3\pm x}S_2$. *Compt. Rendu. Acad. Sci. Paris*, **256**, 3118–20.

Makovicky, E. and Karup-Møller, S. (1993) The system Pd–Fe–S at 900°, 725°, 550°, and 400°C. *Econ. Geol.*, **88**, 1269–78.

Makovicky, E., Barnes, S.-J. and Karup-Møller, S. (1994) PGE containing phase systems and PGE distribution coefficients for magmatic sulfide deposits. *Abstr. 16th General Meeting Internat. Mineralog. Assn. Pisa,* August 1994.

Makovicky, E., Karup-Møller S., Makovicky, M. and Rose-Hansen, J. (1990) Experimental studies on the phase systems Fe–Ni–Pd–S and Fe–Pt–Pd–As–S applied to PGE deposits. *Mineral. Petrol.*, **42**, 307–13.

Makovicky, M., Makovicky, E. and Rose-Hansen, J. (1986) Experimental studies on the solubility and

distribution of platinum group elements in base metal sulphides in platinum deposits. In *Metallogeny of basic and ultra basic rocks* (M.J. Gallagher, R.A. Ixer, C.R. Neary and H.M. Prichard, eds.). London, Inst. Mining Metallurgy, 415–25.

Makovicky, M., Makovicky, E. and Rose-Hansen, J. (1988) Experimental evidence of the formation and mineralogy of platinum and palladium ore deposits. In *Mineral Deposits within the European Community* (J. Boissonnas and P. Omenetto, eds.) Berlin-Heidelberg, Springer-Verlag, 303–17.

Makovicky, E., Rose-Hansen, J., Karup-Møller S. and Makovicky, M. (199?) Factors governing concentration of platinum group elements in layered complexes. *Final Report, parts I-II, Commission of EEC Programme on Primary Raw Materials (Minerals)*. Contract No. MA1M-0006-DK.

Massalski, T.B. (1986) *Binary alloy phase diagrams.* Amer. Soc. Metals, 2 vols, 2224 pp.

Misra, K.C. and Fleet, M.E. (1973) The chemical compositions of synthetic and natural pentlandite assemblages. *Econ. Geol.*, **68**, 518–39.

Moffat, W.G. (1984) *The handbook of binary phase diagrams.* Schenectady, New York, General Electric Co., 3 vols.

Shunk, F.A. (1969) *Constitution of binary alloys*, 2nd supp. New York, McGraw-Hill Book Co., 720 pp.

Skinner, B.J., Luce F.D., Dill, J.A., Hagen, H.A., Lewis, D.M., Odell, D.A., Sverjenski, D.A. and Williams, N. (1976) Phase relations in ternary portions of the system Pt–Pd–Fe–As–S. *Econ. Geol.*, **71**, 1469–75.

Sugaki, A. and Kitakaze, A. (1992) Phase transition of pentlandite. *Abstr. 29th Internat. Geol. Congr. Kyoto,*, **3**, 676.

[*Manuscript received 8 November 1994: revised version accepted 23 March 1995*]